# Review Article: Metal-Organic Frameworks (MOFs) as Adsorbents for Purification of Dye-Contaminated Wastewater: A Review

**Olaniran Kolawole Akeremale***

*Department of Science and Technology Education, Bayero University, Kano, Nigeria*

## A B S T R A C T

Continual and excessive accumulation of coloured contaminants discharged into various water bodies by many industries (textile, leather, paper, dyestuff and plastic) in our environment leading to direct and indirect contamination and pollution of our water system endanger human and aquatic lives. The thermal and photostability nature of these coloured contaminants which makes them difficult to be eliminated from our water system is of great concern. Researchers are continually putting massive attention on the possibilities of improving existing methods and technologies, developing novel strategies, and bring about solutions to subdue these dye-related water contamination problems which will be economically and environmentally friendly. One of the most sustainable technology or method employed in the decontamination and purification of coloured wastewater is adsorption. It possesses several advantages as it has simple and easy design of operation and is highly economical. Metal-organic frameworks (MOFs) play substantial roles under this application as a new class of porous adsorbents that are characterized by a highly crystalline molecular structure and relatively large surface area which is a significant parameter to be considered in adsorption processes. They are also recommended as a good choice of sorbents employed in wastewater purification technologies as a result of their tunable features. This research study aimed at providing a comprehensive review of recent studies on the adsorptive use of MOFs for the removal of these developing organic pollutants from wastewater.

## List of content

*Corresponding Author: Olaniran Kolawole Akeremale (Akeremaleola@gmail.com)*

## 1. Introduction

The rapid increase in the human population, industrialization, and urbanization has brought about a drastic reduction in the quality of water available in our environment [1]. As dyes are the key elements in their everyday manufacturing, the textile, paper, food, and pharmaceutical sectors have been major pollutants of ground and surface water resources, generating a large amount of colored effluents. It is reported that a medium-sized textile industry utilizes about 1.6 million liters of water daily for the production of about 8,000 Kg of fabric [2]. Concerns concerning dye contamination of wastewater have been raised as a result of their obvious colors and persistence in water bodies, and numerous methods have been developed to remove these dye molecules from wastewater prior to their discharge into the environment, the methods include physical, chemical and biological methods [3-4]. Synthetic dyes react with other chemicals to form non-degradable by-products which possess several health hazards [5]. Organic materials such as dye fixing agents that are formaldehyde-based, non-biodegradable dyeing chemicals are highly carcinogenic and mutagenic chemicals [6]. Rag et al. [7] revealed that azo dyes are directly linked to bladder cancer in people, splenic sarcomas, and hepatocarcinoma, which is the principal cause of chromosome aberration in mammalian cells, in their experimental research on the animal model. Malachite green, a prominent carcinogenic material has been shown to cause serious effects on the reproductive and immune systems of humans [8]. Dyes tend to possess a high thermal and photostability; hence, they tend to persist in water if left untreated [9]. Adsorption as a method of purification for the removal of dangerous organic and inorganic components in wastewater is regarded as efficient because of its simple operation, effectiveness, and cost-efficiency [10-11]. Metal-organic frameworks (MOFs) as porous materials have attracted a lot of interest from researchers in the search for more effective adsorbents [12]. The use of MOFs for dye adsorption suggests a low-cost and effective alternative [13]. MOFs are a new category of materials that are defined by their porosity and have been explored over the past 20 years [14]. These materials possess unique properties such as high thermal stability, large surface areas which is a major factor to be considered in adsorption, variable pore sizes, and changeable metal sites [15-16]. MOFs of different sizes can be made in different ways from a wide range of ligands and metal nodes [17-18]. The effectiveness of MOFs for the removal of dye molecules from coloured wastewater has been identified over the past few decades. A separate class of organic dye molecules is stated to be adsorbable on the surfaces of MOFs, regardless of their chromophoric backbones [19].

## 2. Organic dyes' impact environment

Synthetic complex organic and inorganic dyes are mainly made up of hazardous components, which have poor health consequences [11]. Because of their high stability (thermal and photostability), these dyes are resistant to biodegradation, making them difficult to remove using traditional methods [20]. Organic dyes in our water bodies tend to sabotage hydrophytes'

photosynthetic processes by obstructing sunlight penetration, causing harmful compounds to be synthesized [21]. Azo dyes have been linked to multiple forms of cancer cells in several organs, including the liver, bladder, lungs, and spleen, as well as typical abnormalities in model organisms [22]. Dyes containing wastewater discharged as effluents from textile industries induce corrosive traits, decreased dissolved oxygen in water, introduce their unpleasant spell and increase insoluble materials in water. Colloids present in the effluents when discharged into freshwater bodies also bring about a change in their turbidity [23]. Nitrates, nitrites, starch, and sulfides present in these coloured effluents bring about a change in the quantity of dissolved oxygen [24]. The human eyes, skin, and respiratory systems can be affected by acidic dyes as well as initiate cancer cells in humans as a result of their mutagenic nature. Basic dyes on the other hand can cause an increase in heart rate, vomiting, tissue necrosis, jaundice [25]. Textile industries utilize a variety of chemicals, which cause changes in the pH of the water system, harming aquatic species' lives [26]. Effluents from textile industries used in irrigation also pose a threat to plant lives by decreasing their chlorophyll content, plant protein, and carbohydrates [27].

## 3. Treatment methods for dyes containing wastewater

Biological, physical, and chemical approaches are the most common ways for removing organic dyes from industrial effluents. Biological processes can be carried out in both aerobic and anaerobic environments, and they can be utilized to treat both home and industrial waste. Physical processes usually involve suspended rather than dissolved pollutants. Chemical techniques, such as oxidizing organic dye compounds using ozone or hydrogen peroxide or employing an adsorption process, can also be used to decolorize industrial effluents [28]. Presently, the development of potent, economical, effective, and environment-friendly methods of treatment for coloured wastewater from textile and other organic dye using industries is of great concern. These methods could be physio-chemical (physical and chemical), biochemical and at times a combination of both methods is employed to design an effective method for treatment of these effluents. Physical and chemical methods have proven to be highly cost-effective and eco-friendly in recent times [29]. Physical adsorption is generally considered to be the most effective method for quick removal of dissolved dyes in an effluent amongst those methods as a result of its simple operation and effectiveness [10]. In respect to these, activated carbon is commonly known as the most efficient adsorbent for the removal of dyes from coloured industrial effluents. It possesses a large surface area and high adsorption capacities [30]. Regardless of how well activated carbon works as an adsorbent in the treatment of colored wastewater, its use remains very expensive as the adsorbent itself is highly expensive and also has a high regeneration cost when used. As a result of these facts, the quest for relatively cheap alternatives for activated carbon has attracted a growing interest [31]. **Figure 1** shows various class of treatment options available for dyes-contaminated wastewater.
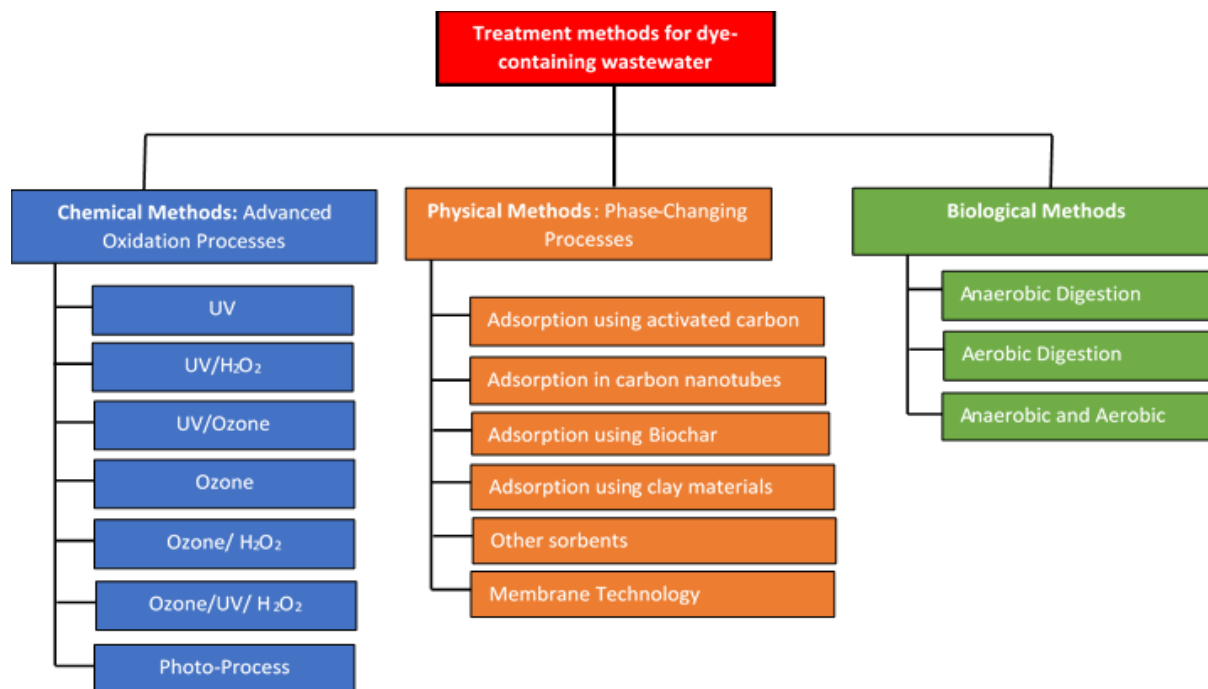
**Figure 1.** Schematic diagram of treatment methods for dyes containing wastewater [32]

### 3.1 Adsorption as a dye removal method

Adsorption can be described as a natural phenomenon where constituents of a liquid or a gas are adhered onto the surface of a solid material. The process of adsorption can be physical or chemical in nature. It is a method that is commonly employed in the treatment of domestic and industrial wastewater. The adherence of particles wastewater onto the surface of adsorbents could be physical or chemical in nature i.e. Physisorption and chemisorption. Physisorption occurs when the intermolecular attractive forces between the adsorbent and adsorbate particles are greater than those between the adsorbate particles themselves. Therefore, physisorption is synonymous to condensation, which involves the emission of heat hence, exothermic in nature. The transport of electrons between the adsorbate and the adsorbent is typical of chemisorption. Chemisorption occurs at temperatures above the adsorbate's critical temperature because it involves chemical bonding between the adsorbate and the adsorbent's surface. Chemical adsorption, like other chemical processes, necessitates activation energy. In addition, chemisorbed species are more confined on the surface than physisorption, and adsorbate molecule movement at the surface is constrained. Adsorption has a number of advantages, including ease of design, cost-effectiveness, safety, simplicity of operation, and resistance to harmful compounds. It is noteworthy that the cost characteristic of adsorption is concerning the cost of the adsorbent employed in the process [33-34]. The surface area of the adsorbent is a major determinant of the extent to which the adsorption process will proceed, hence, tiny particles exhibiting high porosity are essentially required for adsorption in industrial applications. A schematic diagram of the mechanism or adsorption process, where the adsorbate particles are adhered to the surface of the adsorbent is shown in **Figure 2** [35].
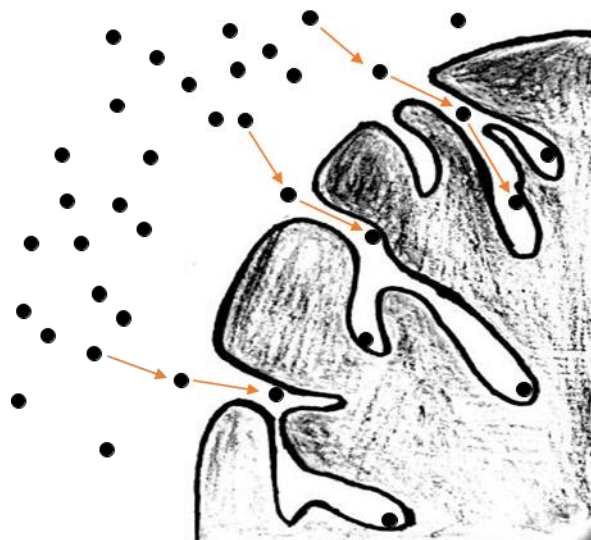
**Figure 2.** Mechanism of adsorption process

Over the past decade, the adsorption technique as a method for wastewater treatment has become quite relevant as a result of its efficiency in removing pollutants that are too stable for biological methods of purification.

### 3.1.1 Adsorption isotherm models commonly used in dyes removal

### 3.1.1.1 Freundlich adsorption isotherm model

The Freundlich model is an empirical adsorption model that can be employed to investigate the adsorption or equilibrium data into heterogeneous surfaces. It is applicable to mono- and multilayer sorption [36]. The Freundlich isothermal model is an empirical equation that describes the interactions between adsorbate and adsorbent on a heterogeneous surface with adsorbing particles with varying adsorption affinities [37]. The linear form of this model is expressed by the following equation [38];

$$(1) \qquad \mathrm{In}q_e = \mathrm{In}K_f + \frac{1}{n}\mathrm{In}C_e$$

Where $q_e$ is the adsorptive capacity which is the quantity of the material adsorbed per unit gram of the adsorbent (mg/g), $C_e$ is the equilibrium adsorbate concentration (mg/L); $K_F$, the Freundlich isotherm constant related to adsorption capacity (indicating the quantity of dye adsorbed onto the adsorbent) and n, the Freundlich isotherm constant related to adsorption intensity (which indicates the

favorability of the adsorption process) can be obtained from the intercept and slope of the plot respectively [38]. Therefore, the plot of $\mathrm{In}q_e$ versus $\mathrm{In}C_e$ will give a straight line of slope $1/n$ and intercepts $\mathrm{In}K_f$.

### 3.1.1.2 Langmuir adsorption isotherm model

Langmuir [39] proposed the Langmuir adsorption model, which describes sorption on homogenous surfaces where micropollutants have a high sorption affinity and form monolayers with particular adsorbent sorption sites [40]. The linear form of the Langmuir's isotherm model is expressed in equation (2);

$$(2) \qquad \frac{C_e}{q_e} = \frac{1}{K_L q_m} + \frac{C_e}{q_m}$$

Where $q_m$ the maximum value of adsorptive capacity (mg/g), $K_L$, is the Langmuir constant (L/mg) which is related to the energy of adsorption are obtained from the intercept and slope of the plot respectively. The constants $q_m$ and $K_L$ were calculated from the slope and intercept of the linear plot of $C_e/q_e$ versus $C_e$ [41].

### 3.1.1.3 Temkin adsorption isotherm model

Temkin [42] also proposed the Temkin isotherm equation as an adsorption model, which posits that adsorption is a multi-layer process with uniform aggregation of binding energies up to maximum binding energy [42]. On account of adsorbate-adsorbent interactions in the adsorption process, it is assumed that the

heat of adsorption of aggregation molecules of adsorbate in the layer reduces linearly with increase in surface coverage [43-44]. Furthermore, during the adsorption process, the model overlooks the comparatively high and low concentrations of the adsorbate in the liquid phase [45]. The linear form of the Temkin isotherm model is given in equation (3);

(3) $$q_e = B\ln A_T + \left[\frac{RT}{b_T}\right]\ln C_e$$

Where: $A_T$ is the equilibrium binding constant [L/g], $b_T$ is the adsorption constant [J/mol K], R is the universal gas constant (8.314 J/mol K), T

is absolute temperature value [298 K], B is a constant related to the heat of sorption [J/mol].

### 3.1.2 Metal-Organic frameworks

Metal-organic frameworks (MOFs) are high-porosity coordination entities made up of inorganic-organic hybrid components. They're a new type of crystalline substance with strong covalent connections that hold them together. MOFs are made up of metal center atoms that serve as connectors and organic ligands that serve as linkers [46-47]. **Figure 3** depicts the fundamental structure of MOFs containing ligands (linkers) and metal ions.
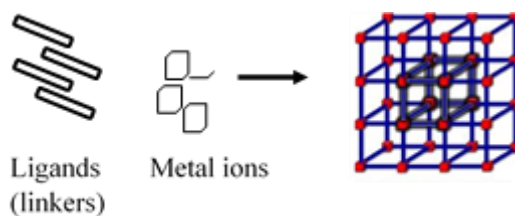


**Figure 3.** Basic structure of MOF

MOFs are known to possess a large pore surface area, including micro-and mesopores, pore shape, pore size, and the surface can be designed in various ways to suit the desired purpose [12,48]. These properties possess several advantages in using MOFs as sorbents in wastewater treatment for emerging contaminants vis adsorption and catalysis [49]. MOFs can be produced using a variety of techniques. Solvothermal synthesis, microwave-assisted synthesis, electrochemical synthesis, mechanochemical synthesis, and sonochemical synthesis are the most prevalent. The approaches differ in how they input energy into the synthetic system, resulting in different reaction durations, yield particle size, and shape [50; 17]. As a result of the flexibility of their structures, numerous classes of MOFs with relatively high surface areas, tunable pore sizes, internal surface properties that are adjustable, make these compound make these compounds better than porous carbons [51].

MOFs are good materials with prospects for removal of dyes from coloured wastewater in

the future via adsorption as a result of their relatively high porosity and specific interactions between the adsorbate and adsorbent [52]. MOFs are three-dimensional (3D) in nature, having a large surface area that can reach 10,000 $m^2$/g, which is significantly larger than other carbon-based materials [53].

Oveisi and colleagues [54] developed five MOFs in 2018. These sorbents were named Materials Institute Lavoisiers (MILs) where the metal supply was tetra isopropyl orthotitanate, while the linkers were 1,4-benzene dicarboxylate (BDC) and 2-amino-1,4-benzene dicarboxylate ($NH_2$-BDC). The five materials include MIL-125(Ti), $NH_2$-MIL-125(Ti), MIL-X1 (BDC/$NH_2$-BDC molar ratio: 75/25), MIL-X2 (BDC/$NH_2$-BDC molar ratio: 50/50), MIL-X3 (BDC/$NH_2$-BDC molar ratio: 25/75). The efficiency of these materials was subjected to examination by using it for the adsorption of three dyes for each material; Methylene blue, Basic red 46, and Basic blue 41. The results obtained are presented in **Table 1**.

**Table 1.** Percentage (%) of dye removed by MILs

| Adsorbent | Dye adsorbed (%) | | |
|---|---|---|---|
| | Basic red 46 | Basic blue 41 | Methylene Blue |
| MIL-125(Ti), | 45 | 41 | 39 |
| NH2-MIL-125(Ti) | 99 | 93 | 97 |
| MIL-X1 | 50 | 45 | 43 |
| MIL-X2 | 75 | 80 | 89 |
| MIL-X3 | 79 | 86 | 91 |

According to the results, $NH_2$-MIL-125(Ti) performed better than the other materials. Because the amino unit is present in its lattices, it has the maximum electron density and zeta potential among them. Several process variables, including the adsorbent dose effect, dye concentration change, solution pH change, and adsorption process contact time were investigated. The following deductions were made: (a) The efficiency of the adsorption process increased as the adsorbent dosage was increased because it increased the number of binding sites for the dyes, whereas it decreased as the dye concentration was increased because the number of dye molecules present in the system was greater than the amount of binding sites present for the adsorbents. (b) the process attained equilibrium at in 30 min (c) consequential adjustment of the pH of the system had no effect on the process.

Nickel-based MOF (SCNU-Z1-Cl) with a surface area of 1636 $m^2$/g was employed as an adsorbent by Deng *et al.* [55], in the adsorption of methyl orange, acridine orange, congo red, and methylene blue from water. This material was found to have a high adsorption capacity and more than 90% of the dyes were removed within an hour of contact time (**Table 2**).

**Table 2.** Application of SCNU-Z1-Cl for adsorption of dyes

| Dyes | SCNU-Z1-Cl Adsorption Capacities $Q_0$ (mg/g) |
|---|---|
| Methyl Orange | 285 |
| Acridine Orange | 180 |
| Congo Red | 582 |
| Methylene Blue | 262 |

Haque *et al.* [56] also synthesized MOF-235 and applied this material for the removal of both cationic (Methylene blue, MO) and anionic (Methyl Orange, MO) dyes simultaneously. MOF-235, $[Fe_3O(terephthalate)_3(DMF)_3]$ [FeCl], (DMF denotes N, N-dimethylformamide), consists of $Fe_3O$ clusters, which is non-toxic [57]. This material has a positive charge of +1 per molecule which is counter-balanced with [FeCl]. The adsorption capacities of MOF-235 for MO and MB were relatively higher than those observed when these dyes were adsorbed onto activated carbon. The quantity of dyes adsorbed to the surface of the adsorbent slightly increased with increased initial concentration, indicating that the adsorption process is favored with high dye concentration as observed in **Table 3**. Furthermore, the pseudo-second-order kinetic constants ($K_2$) measured for MO adsorption onto MOF-235 were much higher than those observed for MO adsorption on activated carbon. The kinetic constants for MB adsorption on MOF-235 and activated carbon, on the other hand, were nearly identical. The inclusion of the Fe component in MOFs imparts a magnetic property to the compound, which in turn generates a magnetic field that facilitates the separation of the material from the solution following adsorption [58].

**Table 3.** Pseudo-second order kinetic rate constant ($K_2$) with adsorption capacities on MOF-235 and activated carbon at varied Mo and MB initial concentrations

| Adsorbents | Dyes | Pseudo-second-order kinetics constants $k_2$ (gm/g/min) | | | | | | Adsorption capacity Qo (mg/g) |
|---|---|---|---|---|---|---|---|---|
| | | 20 mg/L | | 30 mg/L | | 40 mg/L | | |
| | | $k_2$ | $R^2$ | $k_2$ | $R^2$ | $k_2$ | $R^2$ | |
| MOF-235 | MO | $7.67 \times 10^4$ | 0.999 | $8.79 \times 10^4$ | 0.998 | $9.10 \times 10^4$ | 0.998 | 477 |
| | MB | $9.58 \times 10^5$ | 0.995 | $1.67 \times 10^4$ | 0.993 | $2.18 \times 10^4$ | 0,998 | 187 |
| Activated carbon | MO | $1.95 \times 10^4$ | 0.994 | $2.17 \times 10^4$ | 0.987 | $2.34 \times 10^4$ | 0.981 | 11.2 |
| | MB | $9.71 \times 10^5$ | 0.997 | $1.14 \times 10^4$ | 0.979 | $1.48 \times 10^4$ | 0.972 | 26 |

Zhang *et al*. [59] effectively synthesized a magnetic MOF ($Fe_3O_4$/MIL-53(Al)) and used it to remove Congo red (CR) and methylene blue (MB) from synthetic wastewater. The material was synthesized via the solvothermal method and characterized with a scanning electron microscope (SEM), transmission electron microscope (TEM), X-ray diffraction (XRD), and Fourier transform infrared spectrophotometer (FTIR). $Fe_3O_4$/MIL-53(Al) was reported to have a maximum adsorption capacity of 234.4 mg/g for CR adsorption and 70.8 mg/g for MB adsorption, which is quite superior when compared to other adsorbents reported. It should be noted that activated carbon possesses an adsorption capacity of 99.9 mg/g for CR [60] and 47.62 mg/g for MB [31]. The adsorption of CR was fitted with the Langmuir adsorption isotherm model, indicating mono-layer coverage of the adsorbent by the dye molecules, while MB fitted well with the Freundlich isotherm model, indicating Multilayer coverage of the material. Both dyes also followed the pseudo-second-order kinetic model. The sorption process was greatly influenced by pH, ionic strength of the solutions, and the adsorbent load. The major advantage of this particular material is that it can be regenerated for future use by easily introducing an external magnetic field to remove the material from the adsorbed dyes as a result of its magnetic nature.

A similar magnetic Metal-organic Framework was also prepared by Liu *et al*. [61]. In their study, $Fe_3O_4$/MIL-88A composite was synthesized and its adsorption behavior for bromophenol blue (BPB) in aqueous media was examined. It was observed that this material exhibited a maximum adsorption capacity of about 167.2 mg/g for the removal of BPB, which was relatively higher than that of activated charcoal for the same dye as reported by Iqbal and Ashiq [62]. It also maintained over 90% dye removal even after five cycles of being regenerated.

**Table 4** shows a few MOFs prepared with their corresponding adsorption capacities for different types of dyes.

**Table 4**. Comparison of different types of MOFs with their adsorption capacities for different dyes

| MOF | Dyes Treated | Surface Area (m²/g) | Adsorption Capacity (mg/g) | Reference |
|---|---|---|---|---|
| SCNU-Z$_2$ | Methylene Blue | 960.00 | 455.60 | Yu *et al*., 2019 |
| | Crystal Violet | | 847.40 | |
| | Rhodamine B | | 751.8 | |
| | | | | |
| Ni-BDC MOF | Methylene Blue | - | 73.48 | Ahsan et al., 2020 |
| Ni-BDC MOF@GO | " | | 222.80 | |
| Ni-MOF@CNT | " | | 181.96 | |
| | | | | |

| ZIF-8@CS/PVA-ENF(2) | Malachite Green | Pearl necklace shape | 1000.00 | | Mahmoodi *et al*., 2020 |
|---|---|---|---|---|---|
| | | | | | |
| Zr-MOF(bpy) | Rhodamine B | 2141.88 | 918.90 | | Cui *et al*., 2019 |
| | | | | | |
| $Fe_3O_4$@$SiO_2$@UiO-66-Urea | Rhodamine B | 1044.00 | 183.00 | | Hu *et al*., 2016 |
| Ce(III)-doped UiO-67 | Rhodamine B | 1911.90 | 401.20 | | Yang *et al*., 2020 |
| $Ti_3C_2T_x$MXene | Methylene Blue | 9.00 | 140.00 | | Jun *et al*., 2020 |
| | | | | | |
| SCNU-Zl-CI | Methyl orange | 1636.00 | 285.00 | | Wei *et al*., 2018 |
| POM@UiO-66 | Malachite green | 227 | 190.00 | | Zeng *et al*., 2018 |
| ABim-Zn-MOF | Chicago sky blue | 1.40 | 144.26 | | Sherino *et al*., 2020 |
| CoOF | Acid red 18 | 199.00 | 44.26 | | Trukawka *et al*., 2019 |
| SmBTC | Rose Bengal | 5.90 | 380.00 | | Lee *et al*., 2019 |
| In-TATAB | Acid chrome blue k | 623 | 343.00 | | Liu *et al*., 2020 |

## 4. Dye uptake by metal-organic frameworks and the factors that influence it

Starting dye concentration, solution pH, contact time, temperature, surface area, adsorbent particle size, speed of agitation, adsorbent/dye ratio, presence of interfering ions, and adsorbent dosage are all known to affect the uptake of dyes by MOFS (**Figure 4**). Some of these elements are explored farther down. These characteristics require special care and thought in order for the material to work optimally.
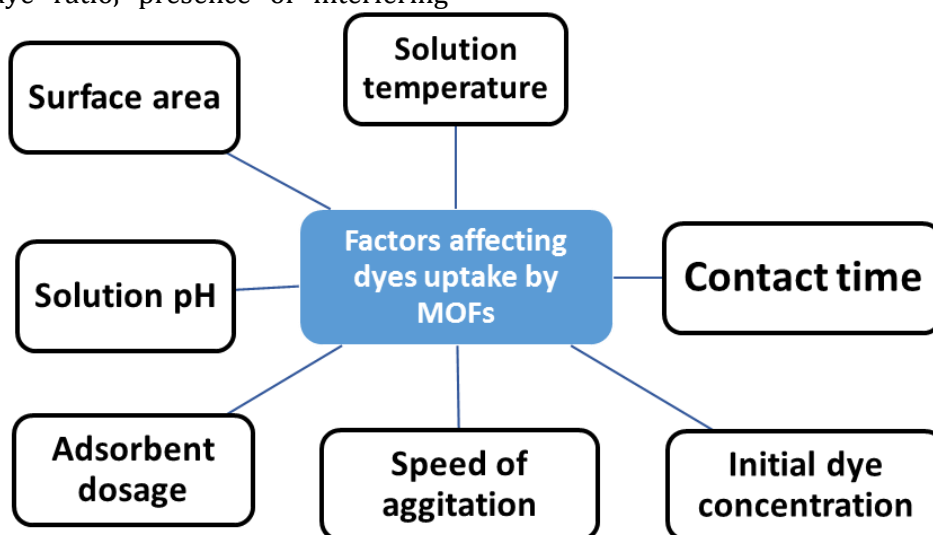


**Figure 4.** Factors affecting dye uptake by MOFs

### 4.1 Adsorbate pH

According to Li *et al.* [63], the pH of the adsorbate has a considerable impact on the adsorption capabilities of adsorbents in taking up dyes, implying that the pH of the solution has a direct impact on dye adsorption effectiveness. The electrostatic charges on the surface of the ionized dye molecules are affected by the pH of the solution, which impacts the rate at which the dye molecules adhere to the surface of the materials [3]. Cationic dyes adsorb better in

solutions with a pH higher than the pH at point of zero charge (pH > pHPZC). The adsorbent's surface is predominantly negatively charged in this state. Also, because the surface of the adsorbent is mainly positively charged, a pH lower than the pH at point of zero charge (pH pHPZC) will favor anionic dye adsorption [64-65]. The pH at the point of zero charge refers to the pH at which the adsorbent's surface has no charge at all (electrically neutral). Depending on the pH of the adsorbate, functional groups on the adsorbent's surface may have a positive or negative charge state [66]. Haque *et al.* [56], employed MOF-235 to remove methyl orange (anionic) and methylene blue from water. The negative charge density of the adsorbent rose as the pH of the solution increased, indicating that it has a higher methylene blue adsorption capability at higher pH. When methyl orange was removed at low pH, the opposite tendency was found (pH of 4). In the adsorption of Rhodamine B and Methylene blue, MOF MIL-68 (Al) was used. The optimal pH for maximal adsorption of these dyes was found to be 6.50 and 7.96, respectively [67].

### 4.2 Initial concentration of dye

Because it impacts the mass transfer of the dye molecules to adsorbent's surface, the initial concentration of the dye adsorbate is a crucial parameter to consider [68]. The concentration of the adsorbate and the number of adsorption sites on the adsorbent's surface determine the adsorbent's maximal adsorption capacity. The rate of adsorption is said to rise with an increase in the initial concentration of the adsorbate because the binding sites on the adsorbent surface get saturated with time [69]. The influence of initial dye concentration on the adsorption process was examined using Uio-66 MOF for the removal of methylene blue. Methylene blue uptake was found to decrease with higher beginning concentrations and rapidly increase with lower initial concentrations. The amount of dye adsorbed was reported to be reduced as a result of repulsion between dye molecules when the surface saturation of the material increased [70].

### 4.3 Adsorbent dosage

The dosage of adsorbents in adsorption processes has been shown in literature to alter the adsorption process. In general, increasing the adsorbent dosage results in the elimination of a large number of dye molecules. This is because as the number of adsorbent binding sites available grows, so does the amount of dye molecules bound to them [71-72]. For the elimination of methyl red, $Fe_3O_4$@MIL-100(Fe) was utilized, and the effect of adsorbent dose was also examined. According to the study, increasing the adsorbent dosage increases the percentage of dyes eliminated. This was made possible by the quantity of binding sites on the adsorbents, which resulted in a relative increase in the adsorbent's surface area [73].

### 4.4 Presence of interfering ions

When external cations and anions are present in the system with the targeted adsorbate (dyes), the MOFs' ability to remove the dyes molecule drastically reduces as these ions compete with the dyes for accessible adsorbent binding sites [74]. Negative anions compete with the anionic dyes of interest while cationic ions when present, cationic dye removal is hindered. According to Wong *et al.* [75], the material's adsorption capacity is reduced due to screening effects on the adsorbent caused by alteration in the electrical double layer caused by an increase in the ionic strength of the solution. It's worth noting that, as seen in the MOFs adsorption of methylene blue, larger ionic concentrations may boost the rate of dye adsorption onto the surface of MOFs. The presence of $Ca^{2+}$ as an interfering ion increased the rate of acid blue adsorption by MOFs [76]. It is recommended that multiple ionic concentrations be tested while treating dye-contaminated wastewater with MOFs.

### 4.5 Speed of agitation

The speed of agitation also has a significant impact on the adsorption process as it controls the level of dye molecule diffusion in the solution and prevents formation of an exterior boundary layer. Under high agitation speed, the thickness of the external layer is considerably reduced, which reduces the dye molecule's barrier to transfer to the MOFs' surface and so increases

the adsorption rate [77]. They also evaluated the adsorption of Remazol deep black RGB (RDB) by MIL-101 MOF, as well as the effect of agitation speed and discovered that increasing the agitation speed improved the RDB adsorption rate, which remained constant at 400rpm. Due to the fact that dye molecule mass transfer is largely the rate-determining step, this makes the speed of agitation to bring about a significant effect on dyes adsorption by MOFs [78].

## 5. Conclusions

MOFs are characterized by their high adaptability, low cost of manufacture, and high efficiency, making them a viable alternative to the more expensive commercial activated carbon. Although extensive research into the different applications of MOFs is currently ongoing, more focus on the use of MOFs as adsorbents for the removal of cationic, anionic, and non-ionic dyes (Emerging Contaminants). is needed. However, while producing novel MOFs to be employed as dye sorbents, the ligand and metal salts to be used in the synthesis of the material must be considered. MOFs are expected to have considerable potential for the treatment of dye-contaminated wastewater due to their improved adsorption capabilities, stability, and comparatively low cost of regeneration.

## Acknowledgment

## Conflict of Interest

The author declares that there is no conflict of interest.

## Orcid

Olaniran Kolawole Akeremale:

https://orcid.org/0000-0002-7677-9589

## References

[1] M.I. Khan, M. Mubashir, D. Zaini, M.H. Mahnashi, B.A. Alyami, A.O. Alqarni, P.L. Show, *J. Hazard. Mater.*, **2021**, *415*, 125364. [Crossref], [Google Scholar], [Publisher]

[2] R.V. Khandare, S.P. Govindwar, *Biotech. Adv.*, **2015**, *33*, 1697-1714. [Crossref], [Google Scholar], [Publisher]

[3] V. Katheresan, J. Kansedo, S.Y. Lau, *J. Environ. Chem. Eng.*, **2018**, *6*, 4676–4697. [Crossref], [Google Scholar], [Publisher]

[4] D. Bhatia, N.R. Sharma, J. Singh, R.S. Kanwar, *Crit. Rev. Environ. Sci. Technol.*, **2017**, *47*, 1836–1876. [Crossref], [Google Scholar], [Publisher]

[5] A. Gurses, M. Acıkyıldız, K. Guneş, M.S. Gurses, *Dyes and Pigments, Springer International Publishing*, **2016**, 69-83. [Publisher]

[6] S. Afroze, T. Sen, M. Ang, *Nova Publishers, USA*, **2015**, 169-213. [Crossref], [Google Scholar], [Publisher]

[7] D.S. Raj, R.J. Prabha, R. Leena, *Jr. Ind. Poll. Cont.*, **2012**, *28*, 57-62. [Google Scholar], [Publisher]

[8] E. Sudova, J. Machova, Z. Svobodova, T. Vesely, *Vet. Med. Praha.*, **2004**, *52*, 527-539. [Crossref], [Google Scholar], [Publisher]

[9] Z. Carmen, S. Daniela, InTechopen., **2012**. [Crossref], [Google Scholar], [Publisher]

[10] M. Abhinaya, R. Parthiban, P.S. Kumar, D.V.N. Vo, *Environ. Res.*, **2021**, *196*, 110996. [Crossref], [Google Scholar], [Publisher]

[11] G. Sharma, T.S. AlGarni, P.S. Kumar, S. Bhogal, A. Kumar, S. Sharma, M. Naushad, Z.A. Alothman, F.J. Stadler, *Environ. Res.*, **2021**, *197*, 111179. [Crossref], [Google Scholar], [Publisher]

[12] G. Li, L. Xia, J. Dong, Y. Chen, Y. Li, *Front. Chem. Eng.*, **2020**, *15*, 285-309. [Crossref], [Google Scholar], [Publisher]

[13] N. A. Khan, Z. Hasan, S. W. Jhung, *J. Hazard. Mater.*, **2013**, *244-245*, 444–456. [Crossref], [Google Scholar], [Publisher]

[14] H.C. Zhou, S. Kitagawa, *Chem. Soc. Rev.*, **2014**, *43*, 5415–5418. [Crossref], [Google Scholar], [Publisher]

[15] Z. Guo, Z. Zhang, Z. Li, M. Dou, F. Wang, *Nanomater. Energy*, **2019**, *57*, 108–117. [Crossref], [Google Scholar], [Publisher]

[16] R. Nivetha, P. Kollu, K. Chandar, S. Pitchaimuthu, S. K. Jeong, A. N. Grace, *RSC Adv.*, **2019**, *9*, 3215–3223. [Crossref], [Google

Scholar], [Publisher]

[17] N. Stock, S. Biswas, *Chem. Rev.*, **2012**, *112*, 933–969. [Crossref], [Google Scholar], [Publisher]

[18] W. Lu, Z. Wei, Z.Y. Gu, T.F. Liu, J. Park, J. Park, *Chem. Soc. Rev.*, **2014**, *43*, 5561–5593. [Crossref], [Google Scholar], [Publisher]

[19] D. Jiang, M. Chen, H. Wang, G. Zeng, D. Huang, M. Cheng, *Coord. Chem. Rev.*, **2019**, *380*, 471–483. [Crossref], [Google Scholar], [Publisher]

[20] A.A. Renita, K.H. Vardhan, P.S. Kumar, P.T. Ngueagni, A. Abilarasu, S. Nath, P. Kumari, R. Saravanan, *Chemosphere*, **2021**, *273*, 129634. [Crossref], [Google Scholar], [Publisher]

[21] H. Wang, J.Q. Su, X.W. Zheng, Y. Tian, X.J. Xiong, T.L. Zheng, *Int. Biodeterior. Biodegradation.*, **2009**, *63*, 395-399. [Crossref], [Google Scholar], [Publisher]

[22] H. Ali, *Water. Soil. Pol.*, **2010**, *213*, 251-273. [Crossref], [Google Scholar], [Publisher]

[23] C. Kemker, Turbidity, total suspended solids and water clarity, *Fondriest Environmental learning center*, 2014. [Publisher]

[24] N.U. Asamudo, A.S. Daba, O.U. Ezeronye, *Afr. J. Biotech.*, **2005**, *4*, 1548-1553. [Crossref], [Google Scholar], [Publisher]

[25] N. Tara, S.I. Siddiqui, G. Rathi, S.A. Chaudhry, A.M.I. Asiri, *Curr. Anal. Chem.*, **2019**, *16*, 14-40. [Crossref], [Google Scholar], [Publisher]

[26] R. Singh, N. Gautam, A. Mishra, R. Gupta, *Ind. J. Pharmacol.*, **2011**, *43*, 246-253. [Crossref], [Google Scholar], [Publisher]

[27] Y. Dessie; S. Tadesse, *J. Chem. Rev.*, **2021**, 3(4), 320-344. [Crossref], [Publisher]

[28] W.T. Tsai, T.Y. Su, K.Y. Lin, C.M. Lin, T.H. Dai, *J. Hazard. Mater.*, **2007**, *147*, 1056–1062. [Crossref], [Google Scholar], [Publisher]

[29] K. Golka, P. Heitmann, F. Gieseler, J. Hodzic, N. Masche, H.M. Bolt, F. Geller, *J. Toxicol. Environ. Health., Part A*, **2008**, *71*, 851-855. [Crossref], [Google Scholar], [Publisher]

[30] S.J. Allen, B. Koumanova, *J. Univ. Chem. Technol. Metallurgy*, **2005**, *40*, 175-192. [Google Scholar], [Publisher]

[31] D. Pathania, S. Sharma, P. Singh, *Arab. J. Chem.*, **2017**, *10*, S1445-S1451. [Crossref], [Google Scholar], [Publisher]

[32] O.M. Rodriguez-Narvaez, J.M. Peralta-Hernandez, A. Goonetilleke, E.R. Bandala, *Chem. Eng. J.*, **2017**, *323*, 361-380. [Crossref], [Google

Scholar], [Publisher]

[33] V. Russo, M. Trifuoggi, M. Di Serio, R. Tesser, *Chem. Eng. Technol.*, **2017**, *40*, 799-820. [Crossref], [Google Scholar], [Publisher]

[34] V. Russo, D. Masiello, M. Trifuoggi, M. Di Serio, R. Tesser, *Chem. Eng. J.*, **2016**, *302*, 287-295. [Crossref], [Google Scholar], [Publisher]

[35] S. Lowell, J.E. Shields, M.A. Thomas, M. Thommes, *Characterization of Porous Solids and Powders: Surface Area, Pore Size and Density, Particle technology Series, Springer, Dordrecht*, **2004**, *16*, 15-57. [Crossref], [Google Scholar], [Publisher]

[36] Y. Vieira, E.C. Lima, E.L. Foletto, G.L. Dotto, *Sci. Total Environ.*, **2021**, *753*, 141981. [Crossref], [Google Scholar], [Publisher]

[37] A.C. Martins, O. Pezoti, A.L. Cazetta, K.C. Bedin, D. A. Yamazaki, G. F. Bandoch, *Chem. Eng. J.*, **2015**, *260*, 291–299. [Crossref], [Google Scholar], [Publisher]

[38] H.F.M. Freundlich, *Z. Phys. Chem.*, **1906**, *57*, 115–124. [Crossref], [Google Scholar], [Publisher]

[39] I. Langmuir, *J. Am. Chem. Soc.*, **1916**, *38*, 2221-2295. [Crossref], [Google Scholar], [Publisher]

[40] J.O. Gonçalves, K.A. da Silva, E.C. Rios, M.M. Crispim, G.L. Dotto, L.A.A. Pinto, *Int. J. Biol. Macromol.*, **2020**, *142*, 85–93. [Crossref], [Google Scholar], [Publisher]

[41] A. Yazidi, M. Atrous, F. E. Soetaredjo, L. Sellaoui, S. Ismadji, A. Erto, *Chem. Eng. J.*, **2020**, *379*, 122320. [Crossref], [Google Scholar], [Publisher]

[42] M.I. Temkin, *Zh. Fiz. Chim.*, **1941**, *15*, 296–332. [Google Scholar], [Publisher]

[43] N. Ayawei, A.N. Ebelegi, D. Wankasi, *J. Chem.*, **2017**, *11.* [Crossref], [Google Scholar], [Publisher]

[44] J. Wang, X. Guo, *Chemosphere*, **2020**, *258*, 127279. [Crossref], [Google Scholar], [Publisher]

[45] O. Hamdaoui, E. Naffrechoux, *J. Hazard. Mater.*, **2007**, *147*, 381–394. [Crossref], [Google Scholar], [Publisher]

[46] C. Hu, X. Hu, R. Li, Y. Xing, *J. Hazard. Mater.*, **2020**, *385*, 121599. [Crossref], [Google Scholar], [Publisher]

[47] P. Cheng, C. Wang, Y.V. Kaneti, M. Eguchi, J. Lin, Y. Yamauchi, J. Na, *Langmuir*, **2020**, *36*, 4231-4249. [Crossref], [Google Scholar], [Publisher]

[48] V.V. Butova, M.A. Soldatov, A.A. Guda, K.A. Lomachenko, C. Lamberti, *Russ. Chem. Rev.*, **2016**, *85*, 280-307. [Crossref], [Google Scholar], [Publisher]

[49] D. Farrusseng, *Wiley Online library*, **2011**, 1-399. [Crossref], [Google Scholar], [Publisher]

[50] M. Yang, Q. Bai, *Colloids Surf.*, **2019**, *582*, 123795 [Crossref], [Google Scholar], [Publisher]

[51] H.C. Zhou, J.R. Long, O.M. Yaghi, *Chem. Rev.*, **2012**, *112*, 673–674. [Crossref], [Google Scholar], [Publisher]

[52] E.M. Dias, C. Petit, *J. Mater. Chem.*, **2015**, *3*, 22484-22506. [Crossref], [Google Scholar], [Publisher]

[53] W.S. Chai, J.Y. Cheun, P.S. Kumar, M. Mubashir, Z. Majeed, F. Banat, S.H. Ho, P.L. Show, *J. Clean. Prod.*, **2021**, *296*, 126589. [Crossref], [Google Scholar], [Publisher]

[54] M. Oveisi, M.A. Asli, N.M. Mahmoodi, *J Hazard. Mater.*, **2018**, *347*, 123-140. [Crossref], [Google Scholar], [Publisher]

[55] S.Q. Deng, X.J. Mo, S.R. Zheng, X. Jin, Y. Gao, S.L. Cai, J. Fan, W.G. Zhang, *Inorg. Chem.*, **2019**, *58*, 2899–2909. [Crossref], [Google Scholar], [Publisher]

[56] E. Haque, J.W. Jun, S.H. Jhung, *J. Hazard. Mater.*, **2011**, *185*, 507–511. [Crossref], [Google Scholar], [Publisher]

[57] A.C. Sudik, A.P. Cote, O.M. Yaghi, Inorg. Chem., **2005**, *44*, 2998–3000. [Crossref], [Google Scholar], [Publisher]

[58] B.E. Meteku, J. Huang, J. Zeng, F. Subhan, F. Feng, Y. Zhang, Z. Qiu, S. Aslam, G. Li, Z. Yan, *Coord. Chem. Rev.,* **2020**, *413*, 213-261. [Crossref], [Google Scholar], [Publisher].

[59] G. Zhang, R. Wo, Z. Sun, G. Hao, G. Liu, Y. Zhang, H. Guo, W. Jiang, *Nanomaterials*, **2021**, *11*, 1917. [Crossref], [Google Scholar], [Publisher]

[60] R. Lafi, I. Montasser, A. Hafiane, *Adsorp. Sci. Technol.*, **2019**, *37*, 160-181. [Crossref], [Google Scholar], [Publisher]

[61] Y. Liu, Y. Huang, A. Xiao, H. Qui, L. Liu, *Nanomaterials*, **2019**, *9*, 51. [Crossref], [Google Scholar], [Publisher]

[62] M.J. Iqbal, M.N. Ashiq, *J. Hazard. Mater.*, **2007**, *139*, 57-66. [Crossref], [Google Scholar], [Publisher]

[63] H. Li, S. Xu, J. Du, J. Tang, Q. Zhou, *RSC Adv.*, **2019**, *9*, 9410-9420. [Crossref], [Google Scholar], [Publisher]

[64] S.E. Olaseni, O.K. Akeremale, C.O. Aboluwoye, *Am. J. Polym. Sci. Technol.*, **2019**, *5*, 16-28. [Crossref], [Google Scholar], [Publisher]

[65] W. Liu, C. Yao, M. Wang, J. Ji, L. Ying, C. Fu, *Environ. Prog. Sustain. Energy*, **2013**, *32*, 655–662. [Crossref], [Google Scholar], [Publisher]

[66] M.S. Nomanbhay, *K. Palanisamy Elect. J. Biotechnol.*, **2005**, *8*, 43-53. [Crossref], [Google Scholar], [Publisher]

[67] M.S. Tehrani, R. Zare-dorabei, *R. Soc. Chem.*, **2016**, *6*, 27416–27425 [Crossref], [Google Scholar], [Publisher]

[68] M. Mhamdi, H. Galai, N. Mnasri, E. Elaloui, M. Trabelsi-Ayadi, *Environ. Sci. Pollut. Res.*, **2017**, *20*, 1686–1697. [Crossref], [Google Scholar], [Publisher]

[69] Y. Bulut, H. Aydın, *Desalination*, **2006**, *194*, 259–267. [Crossref], [Google Scholar], [Publisher]

[70] A.A. Mohammadi, A. Alinejad, B. Kamarehie, S. Javan, A. Ghaderpoury, M. Ahmadpour, M. Ghaderpoori, *Int. J. Environ. Sci. Technol.*, **2017**, *14*, 1959–1968. [Crossref], [Google Scholar], [Publisher]

[71] A. Nasar, F. Mashkoor, *Environ. Sci. Pollut. Res.*, **2019**, *26*, 5333–5356. [Crossref], [Google Scholar], [Publisher]

[72] S. Ahmadi, L. Mohammadi, A. Rahdar, S. Rahdar, R. Dehghani, C.A. Igwegbe, G.Z. Kyzas, *Nanomaterials*, **2020**, *10*, 1–26. [Crossref], [Google Scholar], [Publisher]

[73] S. Dadfarnia, A.M. Haji Shabani, S.E. Moradi, S. Emami, *Appl. Surf. Sci.*, **2015**, *330*, 85–93. [Crossref], [Google Scholar], [Publisher]

[74] A.A. Alqadami, M. Naushad, Z.A. Alothman, T. Ahamad, *J. Environ. Manag.*, **2018**, *223*, 29–36. [Crossref], [Google Scholar], [Publisher]

[75] K.T. Wong, Y. Yoon, S.A. Snyder, M. Jang, *Chemosphere*, **2016**, *152*, 71–80. [Crossref], [Google Scholar], [Publisher]

[76] C.K. Lee, K.S. Low, L.C. Chung, *J. Chem. Technol. Biotechnol.*, **1997**, *69*, 93–99. [Crossref], [Google Scholar], [Publisher]

[77] V. Thi, T. Chau, H.T. Minhthanh, P.D. Du, T. Thanh, T. Toan, T.N. Tuyen, T.X. Mau, D.Q. Khieu, *Hindawi J. Chem.*, **2018,** 1-15. [Crossref], [Google Scholar], [Publisher]

[78] L.W. Lee, S.Y. Pao, A. Pathak, D.Y. Kang, K.L. Lu, *Environ. Sci. Nano.*, **2019**, *6*, 1067–1076. [Crossref], [Google Scholar], [Publisher]

**Olaniran Kolawole Akeremale**: Corresponding author and lecturer with Bayero University kano, Kano State, Nigeria. He Holds a Bachelor of Science degree in Chemistry and Master degree in Physical Chemistry.